

Learning Controls Using Cross-Modal Representations: Bridging Simulation and Reality for Drone Racing

Rogério Bonatti^{*1}, Ratnesh Madaan², Vibhav Vineet², Sebastian Scherer¹, and Ashish Kapoor²

Abstract—Machines are a long way from robustly solving open-world perception-control tasks, such as first-person view (FPV) drone racing. While recent advances in Machine Learning, especially Reinforcement and Imitation Learning show promise, they are constrained by the need of large amounts of difficult to collect real-world data for learning robust behaviors in diverse scenarios. In this work we propose to learn rich representations and policies by leveraging unsupervised data, such as video footage from an FPV drone, together with easy to generate simulated labeled data. Our approach takes a cross-modal perspective, where separate modalities correspond to the raw camera sensor data and the system states relevant to the task, such as the relative pose gates to the UAV. We fuse both data modalities into a novel factored architecture that learns a joint low-dimensional representation via Variational Auto Encoders. Such joint representations allow us to leverage rich labeled information from simulations together with the diversity of possible experiences via the unsupervised real-world data. We present experiments in simulation that provide insights into the rich latent spaces learned with our proposed representations, and also show that the use of our cross-modal architecture improves control policy performance in over 5X in comparison with end-to-end learning or purely unsupervised feature extractors. Finally, we present real-life results for drone navigation, showing that the learned representations and policies can generalize across simulation and reality.

I. INTRODUCTION

First-person view (FPV) racing of drones is an exemplary feat of human mind. Expert pilots are able to plan and control a quadrotor with high agility from a potentially noisy video feed from a monocular camera alone, without comprising the safety of the vehicle. We are interested in exploring the question of what would it take to build an autonomous systems that achieve similar performance levels. This is a difficult problem due to multiple reasons. First, the high dimensional nature and drastic variability of the input image data requires robust representations invariant to visual appearance and artifacts. Second, the image-to-action drone navigation task is a non-myopic sequential decision-making problem, and popular end-to-end control methods such as end-to-end reinforcement and even imitation learning are sample inefficient and/or not robust to perceptual changes in the images [1]–[3]. Lastly, end-to-end training of real-world systems is highly impractical, especially in the initial phases of training when the learnt policy is highly prone to errors and collisions.

¹The Robotics Institute, Carnegie Mellon University, Pittsburgh PA {rbonatti, basti}@cs.cmu.edu

²Microsoft Corporation, Redmond, WA {ratnesh.madaan, vibhav.vineet, akapoor}@microsoft.com

* Work done while interning at Microsoft Corporation, Redmond

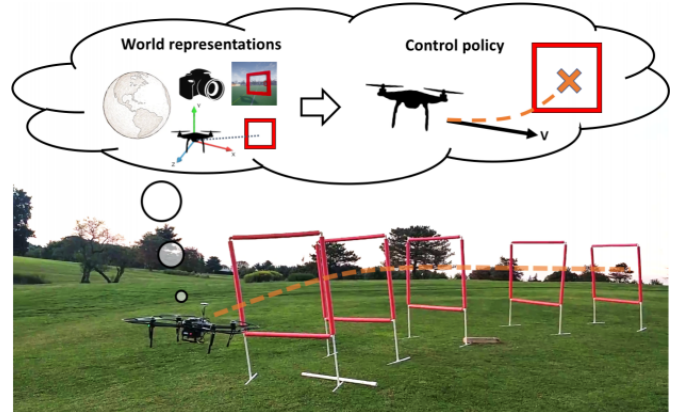


Fig. 1. The proposed framework decouples the control-action loop by first transforming front-facing camera images into a lower-dimensional representation that captures the relevant state, and then using this world representation as an input to a control policy network.

Sim-to-real transfer learning methods aim to alleviate these challenges by training in a synthetic environment and then applying the learnt policies in the real-world [4]–[6]. A key challenge here is that the policy needs to be resilient to appearance and physics differences between simulation and the reality, which is often handled by domain randomization [7], [8]. Collecting labeled real-world data to minimize the sim-to-real gap, albeit possible, requires intensive effort and specialized equipment for gathering ground-truth labels, such as the work of [9], [10] for drone racing.

A key observation in this work is that unsupervised data is relatively easy to gather in real environments. Consequently, a learning framework that can leverage unsupervised first-person-view videos can have a significant advantage. In this paper, we explore the question of combining such unsupervised data which is readily available in real-life, along with labeled simulated data which can be easily generated with high-fidelity simulators [11]. Unsupervised data helps in fine-tuning policies trained only on simulated data, thus helping us bridge the simulation-reality gap. Fig. 1 depicts the overall framework, showing the decomposition of the autonomous navigation into the problems of representation and control policy learning. An autonomous FPV racer drone uses images acquired from a front facing camera to extract a low-dimensional representation pertinent to the racing task. This representation is then used as an input to a control policy network to determine the next control actions.

Our proposed framework entails learning a cross-modal representation for state encoding. The first data modality considers

the raw sensor inputs (FPV images), while the second directly characterizes relevant state information required to solve the task (relative pose of gate defined in the drone frame). We learn a low-dimensional latent representation by extending the cross-modal Variational Auto Encoder (CM-VAE) framework from [12], which uses an encoder-decoder pair for each data modality, while utilizing a single latent space. Consequently, the latent low-dimensional variable can be reconstructed from both modalities, allowing us to incorporate both the labeled and the unlabeled data naturally into the training process. We can then train a control policy using imitation or reinforcement learning that operates over this representation, which is robust across the sim-to-real domain transfer.

While in this paper we specifically focus on the problem of drone racing in the FPV setting, the proposed techniques are general and can be applied to other perception-control robotics tasks. Our key contributions are:

- We present a framework for learning latent state representations for navigation policies that use unsupervised and supervised signals for the same feature extractor;
- We perform detailed experiments and provide insights into the properties of the latent space encoding using variants of the cross-modal framework with simulated and real data;
- We show task performance improvement in learned control policies that use our proposed representations in comparison with end-to-end learning, and show that our training scheme can generalize to real-life navigation.

II. RELATED WORK

a) Navigation policies: Classically, navigation policies rely on state estimation modules that use either visual-inertial based odometry [13] or simultaneous localization and mapping [14]. These techniques can present high drift and noise in typical field conditions, impacting the quality of both the robot localization and the map representation used for planning. Therefore, trajectory optimization based algorithms [15]–[17] can result in crashes and unsafe robot behaviors. Against these effects, [18] learn a collision avoidance policy in dense forests using only monocular cameras, and [19] learn a steering function for aerial vehicles in unstructured urban environments using driving datasets for supervision.

Recently, [20]–[22] explore learning separate networks for the environment representation and controls, instead of the end-to-end paradigm. The goal of an intermediate representations is to extract a low-dimensional space which summarizes the key geometrical properties of the environment, while being invariant to textures, shapes, visual artifacts. Such intermediate representations mean that behavior cloning or reinforcement learning methods have a smaller search space [21] and more sample efficiency.

b) Learning representations for vision: Variational Autoencoder (VAE) based approaches have been shown to be effective in extracting low-dimensional representation from image data [23]–[26]. Recently, VAEs have been leveraged to extract representations from multiple modalities [27]–[30]. Relevant to our work, [30] propose a cross-modal VAE to learn a latent space that jointly encodes different data modalities (images and 3D keypoints associated with hand joints) for an image to hand pose estimation problem.

c) Drone Racing: We find different problem definitions in the context of autonomous drone racing. [8], [9] focus on scenarios with dynamic gates by decoupling perception and control. They learn to regress to a desired position and velocity using monocular images with a CNN, and plan and track a minimum jerk trajectory using classical methods [15], [31]. [8] utilize domain randomization for effective simulation to reality transfer of learned policies [8].

Gate poses are assumed as *a priori* unknown in [32]–[34]. [32] use depth information and a guidance control law for navigation. [33], [34] use a neural network for gate detection on the image. A limitation of the guidance law approach is that the gate must be in view at all times, and it does not take into account gate relative angles during the approach.

[10] formulate drone racing as flight through a predefined ordered set of gates. They initialize gate locations with a strong prior via manual demonstration flights. The belief over each gate location is then updated online by using a Kalman Filter over the gate pose predictions from a neural network.

In our work we combine elements from distinct fields to present a policy learning method that leverages a pre-trained state representation for improved performance. Our cross-modal VAE for training representations exploits easy-to-acquire supervised simulation data along with unsupervised real-world data, improving sim-to-real policy transfer.

III. APPROACH

This work addresses the problem of robust autonomous flight through a set of gates with unknown locations. Our approach is composed of: (1) learning a latent state representation and (2) learning a control policy operating on this latent representation. The first component receives monocular camera images as input and implicitly encodes background features, along with the relative pose of the next visible gate, into a low-dimensional latent representation. This latent representation is then fed into a control network, which outputs a velocity command which is sent to the UAV’s flight controller. Figure 1 depicts the process.

A. Definitions and Notations

We define W as the world frame, B as the body frame, and G_i as the frame of next desired track gate. Let E define the full environment geometry and object categories. Assuming that

all gates are upright, let $y_i = [r, \theta, \phi, \psi]$ define the relative spherical coordinates and yaw of G_i , in the B frame.

We define $q_{RGB}^{\Theta}(I_t) \rightarrow \mathbb{R}^N$ to be an encoder function that maps the current image I_t to a latent compressed vector z_t of size N . Let $\pi^{\Phi}(z_t) \rightarrow \mathbb{R}^4$ be a control policy that maps the current encoded state to a body velocity command $v_B = [v_x, v_y, v_z, v_{\psi}]$, for linear velocities and yaw rate.

Our overall objective is to find the optimal parameters Θ and Φ that minimize the expectation over states s of distance D between our control policy, which operates with partial environment visibility ($q(I)$), and the expert policy π^* , which assumes full knowledge of the environment (E):

$$\Theta^*, \Phi^* = \arg \min_{\Theta, \Phi} \mathbb{E}_s \left[D \left(\pi^*(E), \pi^{\Phi}(q_{RGB}^{\Theta}(I)) \right) \right] \quad (1)$$

B. Learning Cross-Modal Representations for Perception

The goal of the perception system is to create a summary of the current UAV and the environment state E that contains all the relevant task-specific information for the control module. Several approaches exist for features extraction and state representation, from fully supervised to fully unsupervised methods, as mentioned in Section II.

An effective dimensionality reduction technique should be smooth, continuous and consistent [12], and in our application, also be robust across both simulated and real images. To achieve these objectives we build on the architecture developed by Spurr et al. [12], which use a cross-modal derivation of variational auto-encoders (CM-VAE) to train a single latent space using multiple sources of data representation.

CM-VAE derivation and architecture: The cross-modal architecture works by processing a data sample x from different forms into the same latent space location, as seen in Figure 2. In robotics, common data modalities found are RGB or depth images, LiDAR or stereo pointclouds, or 3D keypoints of objects in the environment. In the context of drone racing, we define data modalities as RGB images and the relative pose of the next gate to the current aircraft frame, *i.e.*, $x_{RGB} = I_t$ and $x_G = y_i = [r, \theta, \phi, \psi]$. The input RGB data is processed by encoder q_{RGB} into a normal distribution $\mathcal{N}(\mu_t, \sigma_t^2)$ from which z_t is sampled. Either data modality can be recovered from the latent space using decoders p_{RGB} and p_G .

In the standard definition of VAEs, the objective is to optimize the variational lower bound on the log-likelihood of the data [35], [36]. In [12], this loss is re-derived to account for probabilities across data modalities x_i and x_j , resulting in the new lower bound shown in Eq. 2:

$$\mathbb{E}_{z \sim q(z|x_i)} [\log p(x_j|z)] - D_{KL}(q(z|x_i)||p(z)) \quad (2)$$

We use the Dronet [19] architecture for encoder p_{RGB} , which is equivalent to an 8-layer Resnet [37]. The small size, with about 300K parameters, was chosen for low inference time

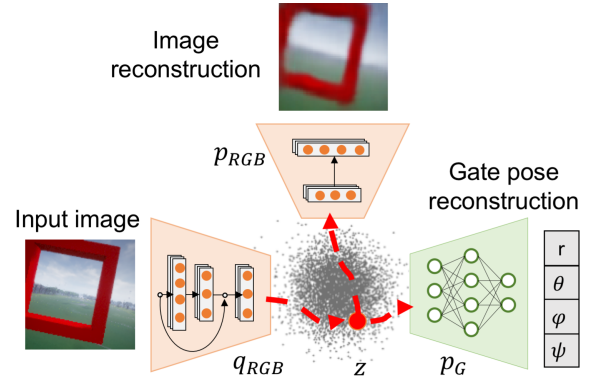


Fig. 2. Cross-modal VAE architecture. Each data sample is encoded into a single latent space that can be decoded back into images, or transformed into another data modality such as for relative gate pose reconstruction.

during deployment. For the image decoder q_{RGB} we use six transpose convolutional layers, and for the gate decoder p_G we use two dense layers.

Training procedure: We follow the training procedure outlined in Algorithm 1 of [12], considering three losses: (i) MSE loss between actual and reconstructed images (I_t, \hat{I}_t), (ii) MSE loss for gate pose reconstruction (y_i, \hat{y}_i), and (iii) Kullback-Leibler (KL) divergence loss for each sample. During training, for each unsupervised data sample we can update networks q_{RGB} , p_{RGB} , and for each supervised sample we update both image encoder q_{RGB} and gate pose decoder p_G using the loss gradients. We detail specific procedures later in Section IV-C.

Imposing constraints on the latent space: Following recent work in disentangled representations [24], [38], we compare two architectures for the latent space structure, with the aim of improving the performance of the control policy and interpretability of the results. The first architecture, z_{unc} , stands for the unconstrained version of the latent space, where: $\hat{y}_i = p_G(z_{unc})$ and $\hat{I}_t = p_{RGB}(z_{unc})$. For second architecture, instead of a single gate pose decoder p_G , we employ 4 independent decoders for each gate pose component. We do this because, as human designers, we know that these features are independent (*e.g.*, the distance between gate and drone should have no effect on the gate's orientation). Therefore, we apply the following constraints to z_{con} : $\hat{r} = p_r(z_{con}^{[0]})$, $\hat{\theta} = p_{\theta}(z_{con}^{[1]})$, $\hat{\psi} = p_{\psi}(z_{con}^{[2]})$, $\hat{\phi} = p_{\phi}(z_{con}^{[3]})$. Image generation still relies on the full latent variable: $\hat{I}_t = p_{RGB}(z_{con})$.

C. Imitation learning for control policy

Expert trajectory planner and tracker To generate expert data ($\pi^*(E)$) we use a minimum jerk trajectory planner following the work of [15], [31], [39] considering a horizon of one gate into the future, and track it using a pure-pursuit path tracking controller. We generate a dataset of monocular RGB images with their corresponding controller velocity commands.

Imitation learning algorithm We use behavior cloning (BC), a variant of supervised learning [40], to train the control

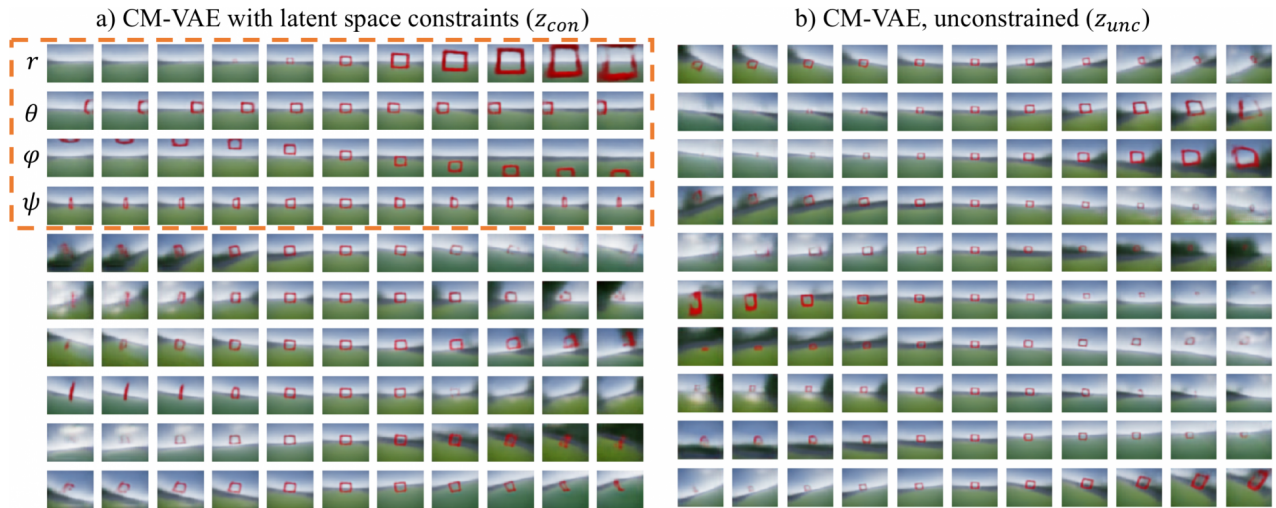


Fig. 3. Visualization of latent space from a) constrained and b) unconstrained cross-modal representations. The constraints on latent space force the first four variables of z_{con} to encode the relative gate pose, condition that is also observed in the image modality.

policy $\pi(q(I))$ when minimizing Equation 1. We freeze all encoder weights when training the control policy. In total we train 5 policies for the simulation experiments in Section IV-B: BC_{con} and BC_{unc} , which operate on z_{con} and z_{unc} respectively as features, BC_{img} , which uses a pure unsupervised image reconstruction VAE for features, BC_{reg} , which uses a purely supervised regressor from image to gate pose as features, and finally BC_{full} , which uses a full end-to-end mapping from images to velocities, without a latent feature vector. We also train BC_{real} on top of the CM-VAE fine-tuned with real data, which is used in Section IV-C.

To provide a fair comparison between policy classes, we design all architectures to have practically the same size and structure. BC policies learned on top of representations are quite small, with only 3 dense layers and roughly 6K neurons. The end-to-end BC_{full} layout is equivalent to the combination of the Dronet encoder plus BC policy from the other cases, but initially all parameters are untrained.

IV. RESULTS

We detail experimental results on learning representations, along with simulation and physical evaluations of the entire system in action. Additional experiments can be found in the supplementary video.

A. Learning Representations

Our first experiments aim to evaluate the latent representations from three different architectures: (i) q_{reg} , for direct regression from $I_t \rightarrow z_{reg} = [r, \theta, \phi, \psi]$, (ii) q_{unc} , for the CM-VAE using RGB and pose modalities without constraints on z : $I_t \rightarrow z_{unc}$, and (iii) q_{con} , for the CM-VAE using RGB and pose modalities with constraints on z : $I_t \rightarrow z_{con}$. We fixed $N = 10$ as the latent space size in all tests.

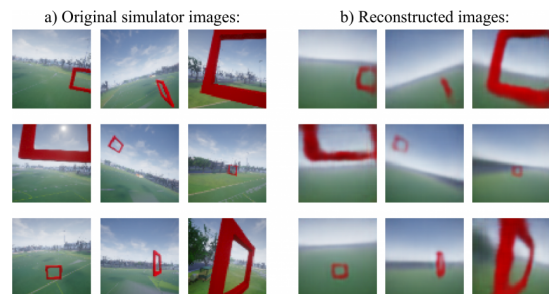


Fig. 4. Comparison between original simulated images with their respective CM-VAE reconstructions. Reconstructed images are blurrier than the original, but overall gate and background features can be well represented.

We generated 300K pairs of 64×64 images and their corresponding ground-truth relative gate poses using the Airsim simulator [11]. We randomly sample the distance to gate, aircraft orientation and gate yaw to generate images, as seen in Figure 4a. 80% of the data was used to train the network, and 20% was used for validation.

Fig. 3 shows an analysis over the images produced by various regions of the latent space decoders from z_{con} and z_{unc} . Each row corresponds to various values of z along one of the 10 latent dimensions. The results highlight that the latent variables can encode relevant information about the gate poses and background information. In addition, we verify that the constrained architecture indeed learned to associate the first four dimensions of z_{con} to affect the size, the horizontal offset, the vertical offset and the yaw of the visible gate.

Fig. 4 depicts examples of input images (left group) and their corresponding reconstructions (right group). We verify that the reconstructions captures the essence of the scene, especially preserving and reconstructing information that's pertinent to the gate poses. Explicit consideration of gate pose recovering with the supervised head enforces that the learned weights preserve this information.

Smoothness of latent space manifold with respect to the gate

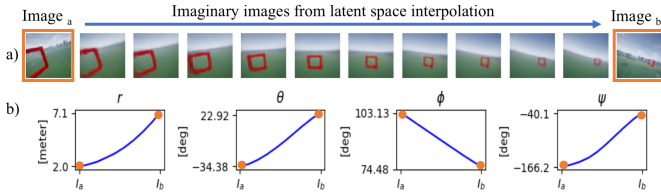


Fig. 5. Visualization of latent space interpolation between two simulated images. Smooth interpolation can be perceived in both data modalities

TABLE I

AVERAGE AND STANDARD ERRORS FOR ENCODING GATE POSES IN DIFFERENT REPRESENTATIONS

q	Radius r [m]	Azimuth θ [°]	Polar ϕ [°]	Yaw ψ [°]
q_{reg}	0.41 ± 0.013	2.4 ± 0.14	2.5 ± 0.14	11 ± 0.67
q_{unc}	0.42 ± 0.024	2.3 ± 0.23	2.1 ± 0.23	9.7 ± 0.75
q_{con}	0.39 ± 0.023	2.6 ± 0.23	2.3 ± 0.25	10 ± 0.75

poses and image outputs is a desirable property (*i.e.*, similar latent vectors correspond to similar gate poses). Intuitively, regularization during training should lead to such smooth latent space representation, and our next analysis confirms that such properties emerge automatically. In Fig. 5 we show the decoded outputs of a latent space interpolation between the encoded vectors from two very different simulated images. Both images and their imagined poses are smoothly reconstructed along this manifold.

Additionally, we evaluate the pose estimates for all three architectures. Table I compares test errors for the three network baselines that can explicitly recover the gate pose. The figure shows that when trained for the same number of epochs until convergence, the cross-modal latent space representations can encode gate pose information better than direct regression, for the same network sizes, likely due to the additional unsupervised gradient information. Figure 6 also shows a detailed histogram of errors in gate pose estimation for the constrained CM-VAE. Overall, the constrained VAE model may be more desirable because in addition to low errors in pose estimation, the latent dimensions are interpretable, making the model more modular and easier to debug.

B. Simulated navigation results

Our next set of experiments evaluates control policies learnt over five different kinds of feature extractors. As described in Section III-C, we train behavior cloning policies on top of the CM-VAE latent spaces (BC_{con} , bc_{unc}), a direct gate pose regressor (BC_{reg}), pure image reconstruction (BC_{img}), and finally full end-to-end training (BC_{full}).

For data collection we generated a nominal circular track with 50m of length, over which we placed 8 gates with randomized position offsets in XYZ, which changed at every drone traversal. We collected 17.5K images with their corresponding expert velocity actions while varying the position offset level from 0-3m. 80%, or 14K datapoints, were used to train the

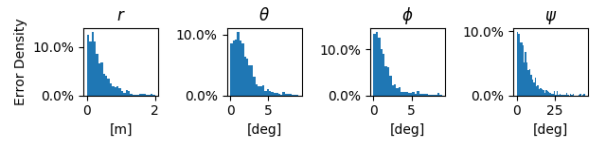


Fig. 6. Histogram showing the density of errors in gate pose decoding for the unconstrained CM-VAE latent representation. Most errors in gate distance are below 0.5m, and the model learned very precise angles for spherical coordinates θ and ϕ . Errors in relative gate yaw are about one order of magnitude higher.

behavior cloning policies, and the remainder were used for validation.

We evaluate of our proposed framework under controlled simulation conditions analogous to data collection. Similarly to previous literature [8]–[10], we define a success metric of 100% as the UAV traversing all gates in 3 consecutive laps. For each data point we averaged results over 10 trials in different randomized tracks. Figure 7 shows the performance of different control policies which were trained using different latent representations, under increasing random position offsets for each gate. At a condition of zero noise added to the gates, most methods, except for the latent representation that uses pure image compression, can perfectly traverse all gates. As the track difficulty increases, end-to-end behavior cloning performance drops significantly, while methods that use latent representations that implicitly or explicitly encode gate poses degrade slower. At a noise level of 3 m over a track with 8 m of nominal radius the proposed cross-modal representation BC_{con} can still achieve approximately 40% success rate, 5X more than end-to-end learning.

C. Real-World Results

We also perform a set of experiments to validate the ability of the cross-modal VAE to combine supervised simulated data and unsupervised real-world images within the same feature extractor, and explore if the behavior cloning policy can be deployed successfully in physical environments. Our drone platform for these tests is a modified DJI M100 quadrotor, as shown in Figure 9. All processing is done with an Intel NUC,

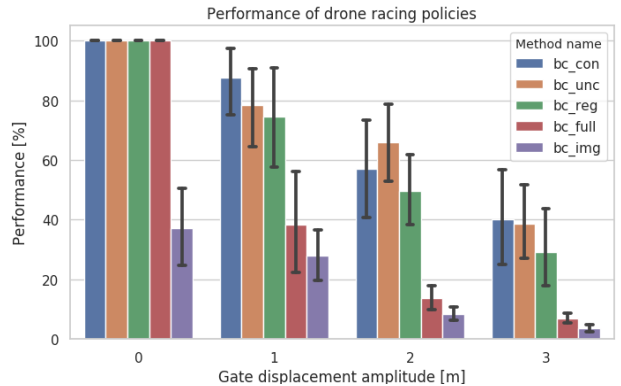


Fig. 7. Performance of different racer policies on simulated track.

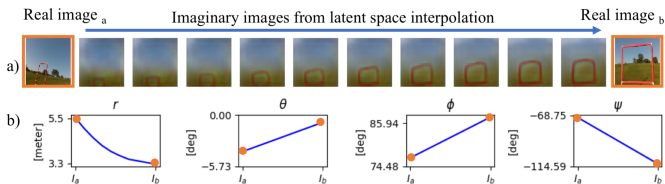


Fig. 8. Visualization of latent space interpolation from real-world images.

with Intel i7 quad-core CPU and 16GB of RAM. An off-the-shelf Intel T265 Tracking Camera provides robot odometry, mounted 45° downwards. The image processing loop runs at 60Hz on the onboard CPU with Tensorflow 2.0.

The objective for the first experiment was to first train a constrained CM-VAE architecture combining real and simulated data. The real-life unsupervised data set was collected in manual UAV flights in an outdoors racing track and consisted of 100K images without any labels.

After training, we display examples of real-life data interpolation in Fig 8, which shows that the latent space encoding z_{real} remains smooth and consistent. The procedure adopted for training was to initially start with the same weights of the constrained CM-VAE trained in simulation, and fine-tune the network, with a smaller learning rate, using data modalities of real images and the supervised component from simulated data, without simulated images this time. We tried different approaches for training, such as training a model from scratch using simulated and real images, but we found that this training procedure tended to decode both data modalities to different regions of the latent space, rendering inconsistent representations.



Fig. 9. Details of the UAV platform used for experiments.

For the second experiment, we trained a behavior cloning policy BC_{real} for navigation using the trained feature extractor q_{real} , and deployed it on a 25m-long segment. Fig. 10 displays samples of the drone’s camera images along with the outputted velocities. Notice that the command outputs appear to be fairly cyclical, which indicates that the policy works myopically for each next gate seen in the image.

V. CONCLUSION AND DISCUSSION

We have presented a framework to solve perception-control tasks that leverages readily available unsupervised real-world data together with simulated supervised training data to learn robust representations in an efficient manner. At the heart of our approach is a cross-modal Variational Auto-Encoder framework that jointly encodes sensor data and useful task-specific state information into a useful latent representation to be leveraged by control policies. We provide simulation studies and real-world experiments that highlight the effectiveness of our framework on the task of FPV

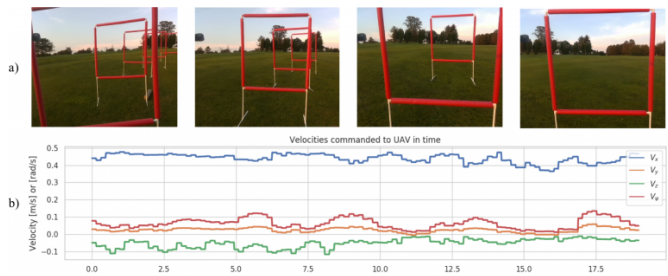


Fig. 10. Visualization of UAV first-person view images along with commanded output velocities. Notice the cyclical pattern in velocities, indicative of a 1-gate myopic policy behavior.

drone racing. Our results show that the use of cross-modal representations significantly improves task performance in comparison with end-to-end approaches.

From our experiments we are able to infer that features trained for unsupervised image reconstruction, which are implicitly encoded in the latent space, can serve as important cues describing the UAV’s current state for the control policy on top of the human-defined supervised parameters. For example, by using background features such as the line of horizon, it may be possible to infer the aircraft’s current banking angle, which influences the commanded velocities. This remark can serve as an additional motivator for the use of a semi-supervised features extraction module, since it is difficult to hand-define all relevant features for a particular control task. Another advantage of the CM-VAE architecture is that it can allow the robot operator to gain insights onto the decisions made by the networks. For instance, a human can interpret the decoded gate pose and decoded images in real time and stop the vehicle if perception seems to be abnormal.

Future work includes extensions of the cross-modal semi-supervised feature extraction framework to other robotic tasks, considering the use of multiple unsupervised data modalities that span beyond images. We believe that applications such as autonomous driving and robotic manipulation present perception and control scenarios analogous to the drone navigation task, where real-world unsupervised data is abundant, and supervised simulated data can be cheaply obtained.

Additionally, we plan to investigate training more complex control policies on top of the learned latent representations, such as with the use of reinforcement learning (RL). To do such, we can obtain more accurate state representations by applying recurrent dynamics models to the features extracted with the CM-VAE, following techniques discussed in [20]. Within the context of RL, we would be interested in comparing our architecture with similar concepts such as the use of auxiliary unsupervised tasks [41].

ACKNOWLEDGMENTS

We thank Matthew Brown, Nicholas Gyde, Christoph Endner, and Lorenz Stangier for the help with the simulation and experimental setups, and Debadepta Dey for insightful discussions.

REFERENCES

- [1] K. Kang, S. Belkhal, G. Kahn, P. Abbeel, and S. Levine, "Generalization through simulation: Integrating simulated and real data into deep reinforcement learning for vision-based autonomous flight," *arXiv preprint arXiv:1902.03701*, 2019.
- [2] L. Tai, G. Paolo, and M. Liu, "Virtual-to-real deep reinforcement learning: Continuous control of mobile robots for mapless navigation," in *2017 IEEE/RSJ International Conference on Intelligent Robots and Systems (IROS)*. IEEE, 2017, pp. 31–36.
- [3] J. Zhu, Z. Zhang, C. Zhang, J. Wu, A. Torralba, J. B. Tenenbaum, and W. T. Freeman, "Visual object networks: Image generation with disentangled 3d representation," *CoRR*, vol. abs/1812.02725, 2018.
- [4] F. Sadeghi and S. Levine, "(CAD)²RL: Real single-image flight without a single real image," *arXiv preprint arXiv:1611.04201*, 2016.
- [5] Y. Ganin, E. Ustinova, H. Ajakan, P. Germain, H. Larochelle, F. Laviolette, M. Marchand, and V. Lempitsky, "Domain-adversarial training of neural networks," *The Journal of Machine Learning Research*, vol. 17, no. 1, pp. 2096–2030, 2016.
- [6] J. Tobin, R. Fong, A. Ray, J. Schneider, W. Zaremba, and P. Abbeel, "Domain randomization for transferring deep neural networks from simulation to the real world," in *2017 IEEE/RSJ International Conference on Intelligent Robots and Systems (IROS)*. IEEE, 2017, pp. 23–30.
- [7] Y. Wu, Y. Wu, G. Gkioxari, and Y. Tian, "Building generalizable agents with a realistic and rich 3d environment," *arXiv preprint arXiv:1801.02209*, 2018.
- [8] A. Loquercio, E. Kaufmann, R. Ranftl, A. Dosovitskiy, V. Koltun, and D. Scaramuzza, "Deep drone racing: From simulation to reality with domain randomization," *arXiv preprint arXiv:1905.09727*, 2019.
- [9] E. Kaufmann, A. Loquercio, R. Ranftl, A. Dosovitskiy, V. Koltun, and D. Scaramuzza, "Deep drone racing: Learning agile flight in dynamic environments," *arXiv preprint arXiv:1806.08548*, 2018.
- [10] E. Kaufmann, M. Gehrig, P. Fohrn, R. Ranftl, A. Dosovitskiy, V. Koltun, and D. Scaramuzza, "Beauty and the beast: Optimal methods meet learning for drone racing," in *2019 International Conference on Robotics and Automation (ICRA)*. IEEE, 2019, pp. 690–696.
- [11] S. Shah, D. Dey, C. Lovett, and A. Kapoor, "Airsim: High-fidelity visual and physical simulation for autonomous vehicles," *Field and Service Robotics*, 2017. [Online]. Available: <https://arxiv.org/abs/1705.05065>
- [12] A. Spurr, J. Song, S. Park, and O. Hilliges, "Cross-modal deep variational hand pose estimation," in *Proceedings of the IEEE Conference on Computer Vision and Pattern Recognition*, 2018, pp. 89–98.
- [13] J. Delmerico and D. Scaramuzza, "A benchmark comparison of monocular visual-inertial odometry algorithms for flying robots," in *2018 IEEE International Conference on Robotics and Automation (ICRA)*. IEEE, 2018, pp. 2502–2509.
- [14] J. Sturm, N. Engelhard, F. Endres, W. Burgard, and D. Cremers, "A benchmark for the evaluation of rgb-d slam systems," in *2012 IEEE/RSJ International Conference on Intelligent Robots and Systems*. IEEE, 2012, pp. 573–580.
- [15] D. Mellinger and V. Kumar, "Minimum snap trajectory generation and control for quadrotors," in *Robotics and Automation (ICRA), 2011 IEEE International Conference on*. IEEE, 2011, pp. 2520–2525.
- [16] H. Oleynikova, M. Burri, Z. Taylor, J. Nieto, R. Siegwart, and E. Galceran, "Continuous-time trajectory optimization for online uav replanning," in *2016 IEEE/RSJ International Conference on Intelligent Robots and Systems (IROS)*. IEEE, 2016, pp. 5332–5339.
- [17] R. Bonatti, C. Ho, W. Wang, S. Choudhury, and S. Scherer, "Towards a robust aerial cinematography platform: Localizing and tracking moving targets in unstructured environments," *2019 IEEE/RSJ International Conference on Intelligent Robots and Systems (IROS)*, 2019.
- [18] S. Ross, N. Melik-Barkhudarov, K. S. Shankar, A. Wendel, D. Dey, J. A. D. Bagnell, and M. Hebert, "Learning monocular reactive uav control in cluttered natural environments," in *IEEE International Conference on Robotics and Automation*. IEEE, March 2013.
- [19] A. Loquercio, A. I. Maqueda, C. R. Del-Blanco, and D. Scaramuzza, "Dronet: Learning to fly by driving," *IEEE Robotics and Automation Letters*, vol. 3, no. 2, pp. 1088–1095, 2018.
- [20] D. Ha and J. Schmidhuber, "World models," *arXiv preprint arXiv:1803.10122*, 2018.
- [21] T. Lesort, N. Díaz-Rodríguez, J.-F. Goudou, and D. Filliat, "State representation learning for control: An overview," *Neural Networks*, vol. 108, pp. 379–392, 2018.
- [22] D. Hafner, T. Lillicrap, I. Fischer, R. Villegas, D. Ha, H. Lee, and J. Davidson, "Learning latent dynamics for planning from pixels," *arXiv preprint arXiv:1811.04551*, 2018.
- [23] M. W. Diederik Kingma, "Autoencoding variational bayes," in *ICLR*, 2014.
- [24] I. Higgins, L. Matthey, A. Pal, C. Burgess, X. Glorot, M. Botvinick, S. Mohamed, and A. Lerchner, "beta-vae: Learning basic visual concepts with a constrained variational framework," in *5th International Conference on Learning Representations, ICLR 2017, Toulon, France*, 2017.
- [25] H. Kim and A. Mnih, "Disentangling by factorising," *arXiv:1802.05983*, 2018.
- [26] C. P. Burgess, L. Matthey, N. Watters, R. Kabra, I. Higgins, M. Botvinick, and A. Lerchner, "Monet: Unsupervised scene decomposition and representation," *CoRR*, 2019.
- [27] Y. Aytar, L. Castrejon, C. Vondrick, H. Pirsiavash, and A. Torralba, "Cross-modal scene networks," *IEEE transactions on pattern analysis and machine intelligence*, vol. 40, no. 10, pp. 2303–2314, 2017.
- [28] J. Ngiam, A. Khosla, M. Kim, J. Nam, H. Lee, and A. Y. Ng, "Multimodal deep learning," in *Proceedings of the 28th international conference on machine learning (ICML-11)*, 2011, pp. 689–696.
- [29] V. E. Liang, J. Lu, Y.-P. Tan, and J. Zhou, "Cross-modal deep variational hashing," in *2017 IEEE International Conference on Computer Vision (ICCV)*. IEEE, 2017, pp. 4097–4105.
- [30] A. Spurr, J. Song, S. Park, and O. Hilliges, "Cross-modal deep variational hand pose estimation," in *The IEEE Conference on Computer Vision and Pattern Recognition (CVPR)*, June 2018.
- [31] C. Richter, A. Bry, and N. Roy, "Polynomial trajectory planning for aggressive quadrotor flight in dense indoor environments," in *Robotics Research*. Springer, 2016, pp. 649–666.
- [32] S. Jung, S. Cho, D. Lee, H. Lee, and D. H. Shim, "A direct visual servoing-based framework for the 2016 iros autonomous drone racing challenge," *Journal of Field Robotics*, vol. 35, no. 1, pp. 146–166, 2018.
- [33] S. Jung, S. Hwang, H. Shin, and D. H. Shim, "Perception, guidance, and navigation for indoor autonomous drone racing using deep learning," *IEEE Robotics and Automation Letters*, vol. 3, no. 3, pp. 2539–2544, 2018.
- [34] S. Jung, H. Lee, S. Hwang, and D. H. Shim, "Real time embedded system framework for autonomous drone racing using deep learning techniques," in *2018 AIAA Information Systems-AIAA Infotech Aerospace*, 2018, p. 2138.
- [35] D. P. Kingma and M. Welling, "Auto-encoding variational bayes," *arXiv preprint arXiv:1312.6114*, 2013.
- [36] D. J. Rezende, S. Mohamed, and D. Wierstra, "Stochastic backpropagation and approximate inference in deep generative models," *arXiv preprint arXiv:1401.4082*, 2014.
- [37] K. He, X. Zhang, S. Ren, and J. Sun, "Deep residual learning for image recognition," in *Proceedings of the IEEE conference on computer vision and pattern recognition*, 2016, pp. 770–778.

- [38] H. Kim and A. Mnih, "Disentangling by factorising," *arXiv preprint arXiv:1802.05983*, 2018.
- [39] M. Burri, H. Oleynikova, M. W. Achtelik, and R. Siegwart, "Real-time visual-inertial mapping, re-localization and planning onboard mavs in unknown environments," in *Intelligent Robots and Systems (IROS 2015), 2015 IEEE/RSJ International Conference on*, Sept 2015.
- [40] T. Osa, J. Pajarinen, G. Neumann, J. A. Bagnell, P. Abbeel, J. Peters *et al.*, "An algorithmic perspective on imitation learning," *Foundations and Trends® in Robotics*, vol. 7, no. 1-2, pp. 1–179, 2018.
- [41] M. Jaderberg, V. Mnih, W. M. Czarnecki, T. Schaul, J. Z. Leibo, D. Silver, and K. Kavukcuoglu, "Reinforcement learning with unsupervised auxiliary tasks," *arXiv preprint arXiv:1611.05397*, 2016.